PHYSICAL REVIEW B VOLUME 15, NUMBER 4 15 FEBRUARY 1977

Renormalized atoms: Cohesion in transition metals

C. D. Gelatt, Jr.*
Physics Department, Harvard University, Cambridge, Massachusetts 02138

H. Ehrenreich*
Division of Engineering and Applied Physics, Harvard University, Cambridge, Massachusetts 02138

R. E. Watson†
Brookhaven National Laboratory, Upton, New York 11973
(Received 19 July 1976)

The renormalized-atom method is used to calculate the cohesive energy of the $3d$ and $4d$ transition-metal elements and the equilibrium lattice constant and bulk modulus of two representative elements, Ti and Cu. The results agree with experiment to within 20% for most elements. The method of calculation allows the cohesive energy to be decomposed into a number of contributions whose relative importance can be investigated both as a function of valence and as a function of density. No evidence of d-d repulsion is found for the transition or noble metals. Instead the "spring" which holds the atoms apart is the result of the increasing kinetic energy of the conduction electrons as the density is increased. The d-d interaction is uniformly attractive and produces the minimum in the Wigner-Seitz radius near the center of a transition-metal period. Band structures calculated from renormalized-atom and $X\alpha$ potentials are compared and the relationships among them are discussed in some detail.

I. INTRODUCTION

With a few notable exceptions, theoretical work concerning the cohesive energy of transition metals did not represent a major effort until the advent of large-scale computers. This situation should be contrasted with the systematic efforts for alkali metals.[1,2] Fuchs[3] was the first to calculate the cohesive energy of a transition metal using the Wigner-Seitz technique. In his work on copper he assumed the d bands could be treated as core states. Hartree free-atom wave functions and potentials were used and the effects of exchange were taken into account to first order in perturbation theory. His results yielded essentially the correct equilibrium density and cohesive energy, but the bulk modulus was too small by a factor of 4. Fuchs postulated that this error was due to the neglect of exchange repulsion between the filled copper d shells, an effect which this paper will show to be absent. Estimating this repulsion with a modification of the Thomas-Fermi model he was able to reproduce the experimental bulk modulus, but the calculated density was 20% too high and the binding energy was only 50% of the experimental result. Similar results were obtained by Kambe[4] 20 years later using the quantum defect method to generate the effective crystal potential. In both cases it was assumed that the use of atomic potentials was sufficient for calculations of the cohesive energy of solid.

Stern[5] performed very careful calculations for Fe which included investigations of the equilibrium valence-electron configuration and band-structure effects. Exchange contributions were neglected and the s and d bands were treated as separate and noninteracting. (The first band calculations to include s-d hybridization effects fully were those of Segall[6] and Burdick[7] for copper.) In spite of these approximations the calculated Wigner-Seitz radius, cohesive energy, and bulk modulus were all in excellent agreement with experiment. Furthermore, Stern found it unnecessary to include an *ad hoc* core-core repulsion term.

One of the key puzzles was why the cohesive energy of Cu was approximately twice as large as that of K which also has only a single electron outside closed shells. Van der Waals interactions among d shells[8] as well as s-d hybridization effects[9] were postulated as sources for this increased cohesive energy in the noble metals. Wigner[1] and Friedel[10] pointed out that in the case of transition metals the formation of a partially filled d band accounts for the general parabolic trend of the cohesive energy across a transition-metal row. This observation was justified in greater detail by later calculations of Ducastelle and Cyrot-Lackmann.[11] In the same spirit, Kollar and Solt[12] attempted to calculate the trends of cohesive properties across the $3d$ and $4d$ rows using a model which rather crudely grafted together a nearly-free-electron conduction band and a tight-binding d band, but neglected s-d hybridization. The agreement with experiment was qualitatively reasonable, but not quantitative.

More recently there have been a number of de-

tailed self-consistent calculations of transition-metal cohesive energies.[13] Although such calculations represent the current state of the art and yield reasonable agreement with experiment, it is difficult to dissect them in order to obtain physical insight about which components of the cohesive energy are the most important.

The calculations reported in this paper bridge the gap between *ad hoc* models and the most sophisticated state of the art calculations. They are based on the renormalized-atom method for calculating structure-independent properties of transition metals, which was introduced in a previous series of papers.[14-16] The method provides both a technique for generating an effective one-electron potential for a metal from atomic wave functions and a means of estimating gross features of the band structure and cohesive energy without the necessity of performing detailed band calculations. While the principal justification for this view comes from a comparison of renormalized-atom and band calculation results, some other aspects, for example, the approximations used to calculate the band limits of the d and conduction bands of transition metals, have been discussed explicitly by Andersen.[17]

The adequacy of the renormalized charge density obtained from this approach has been substantiated by the work of Berggren and coworkers[18] on the electron momentum distribution determined from Compton profiles. For the two elements studied, Ti and V, the renormalized-atom electron momentum distribution is significantly superior to that for the free atom. In fact, the renormalized-atom results agree with experiment essentially within the statistical accuracy of the measurements and thus obviate the use of explicit band calculations.

The present calculations include the full effects of band formation on the sum of one-electron energies. The placement of the bands is such as to produce substantially good agreement with experiments measuring one-electron excitations. However, the calculations themselves are not self-consistent. The double counted two-electron terms in the metal are calculated using renormalized-atom wave functions rather than band eigenstates. The calculations have the advantage of being structured in such a way that it is possible to separate the energy of formation of the metal starting from free atoms into a number of terms and examine the importance of each, in particular its dependence on atomic radius and valence.

Section II reviews and extends the renormalized-atom method for estimating band energies without carrying out a full band calculation. Section III presents a complete set of calculations of the cohesive energy of the $3d$ and $4d$ transition metals at their experimental density. The results improve upon the previously published[15] renormalized-atom estimates. Section IV extends the cohesive-energy calculations to calculation of the equilibrium Wigner-Seitz radius and the bulk modulus for K, Cu, and Ti. Section V presents a simple explanation of the trend of the equilibrium radius across the transition-metal rows. This explanation is supported by a calculation of the equilibrium Wigner-Seitz radius of all $3d$ metals based only on the density dependence of the band structure of Cu.

Appendix A reviews the construction of the renormalized-atom potential. A detailed comparison is made between this method and the common technique[19] of overlapping free-atom Hartree potentials and using a Slater[20] $\rho^{1/3}$ exchange potential, and the origin of the differences is discussed. Appendix B presents a detailed description of the cohesive-energy calculations.

II. BAND-STRUCTURE INFORMATION FROM RENORMALIZED ATOMS

One of the goals of the renormalized-atom method is to abstract the structure-independent properties of metals without the computational cost of a full band-structure calculation. In particular, one would like to know the limits of the spectrum of eigenvalues of states of a particular character, such as the energy of the bottom of the conduction band, the location of the top and bottom of the d band in a transition metal, and the Fermi energy. Approximate values for these quantities can be determined from the single-site potential without making use of the periodic structure of the solid.[16]

The construction of the renormalized-atom potential given the atomic wave functions is described in Appendix A. To summarize, the atomic valence wave functions are truncated at the Wigner-Seitz radius (defined by $4\pi R_{\mathrm{WS}}^3/3 = V/N$ where V/N is the volume per atom) and multiplied by a normalization constant within R_{WS}:

$$R_{nl}(r) = \begin{cases} N_{nl} R_{nl}^{\mathrm{atomic}}(r), & r \leq R_{\mathrm{WS}} \\ 0, & r > R_{\mathrm{WS}} . \end{cases} \tag{1}$$

Here R_{nl}^{atomic} is the atomic radial wave function for the state with quantum numbers n and l, and N_{nl} is defined by

$$N_{nl}^{-2} = \int_0^{R_{\mathrm{WS}}} [R_{nl}^{\mathrm{atomic}}(r)]^2 r^2 \, dr . \tag{2}$$

A single-site l-dependent crystal potential is constructed from these wave functions just as the free-atom Hartree-Fock potential is generated from atomic wave functions. This implies the use of the nucleus-centered Wigner-Seitz ex-

change-correlation hole which eliminates the self-Coulomb interaction: an electron at a neutral site with nuclear charge Z sees the potential due to the $Z-1$ *other* electrons with different quantum numbers on the same site. The Hartree localized exchange approximation[21] is used to eliminate the energy dependence of the exchange term.

In Appendix A the renormalized-atom-potential band structure of Cu is compared with results calculated from overlapping-atom potentials using either the Slater[20] or Kohn-Sham[22] forms of the local exchange potential. It is seen that there are significant differences among these results in the placement of the bands relative to the atomic zero of potential and relative to each other. The most basic cause of these differences is the radial dependence of

$$\delta\rho(r)=\rho^{\text{solid}}(r)-\rho^{\text{atom}}(r),$$

where ρ^{solid} and ρ^{atom} are the charge densities of the solid and the free atom. The renormalized atom yields an essentially constant $\delta\rho(r)$ while the overlapping-atoms prescription leads to a $\delta\rho(r)$ strongly peaked in the outer regions of a Wigner-Seitz cell. The greater screening for the renormalized atom results in d bands which lie higher relative to the conduction band. This Hartree potential difference can be offset by varying the strength of the $\rho^{1/3}$ exchange potential. Since it is stronger in the small-radius region where the amplitude of the d wave functions is large, scaling down the strength of the exchange potential also raises the d bands relative to the conduction bands. Finally, the methods make a different choice of the zero of the Hartree potential which leads to the different placement of the bands relative to the atomic zero.

As was shown previously,[16] the energy of the bottom of the conduction band (bonding s level) and the bottom and top of the d band (bonding and antibonding d levels) can be determined to within a few hundredths of a rydberg from appropriate boundary conditions applied at the Wigner-Seitz radius.

For bonding states,

$$\frac{d}{dr}[R_l(R_{\text{WS}},\epsilon_{\text{min}})]=0, \tag{3}$$

for antibonding states,

$$R_l(R_{\text{WS}},\epsilon_{\text{max}})=0. \tag{4}$$

As an example, Fig. 1 shows the Cu logarithmic derivatives, $R_l^{-1}(dR_l/dr)$, evaluated at the Wigner-Seitz radius for angular momentum $l=0$ to 2 plotted versus energy. For fcc crystals the bonding s and p levels correspond to states of Γ_1 and L_2' symmetry, respectively, while the bottom and

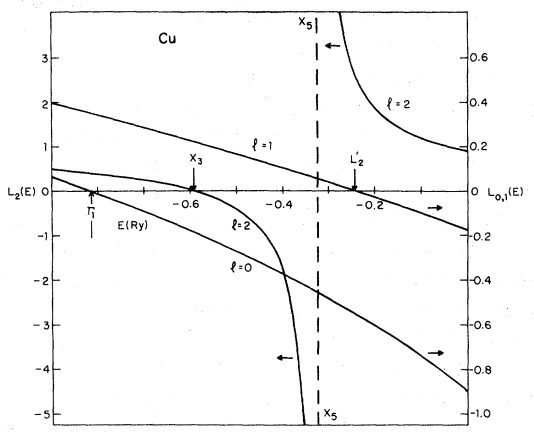

FIG. 1. Logarithmic derivatives evaluated at the Wigner-Seitz radius of the renormalized-atom Cu potential for $l=0,1,2$ plotted vs energy. The zeros and singularities of $L_l(E)$ determine the band extrema. Note the compressed vertical scale for $l=2$.

top of the unhybridized d band correspond to bonding and antibonding states having X_3 and X_5 symmetry. The arrows in Fig. 1 denote the location of bonding states, and the asymptote that of the antibonding d state.

An approximate value for the Fermi energy can be calculated from the phase shifts of the single-site potential. Lloyd[23] has derived an expression for the integrated density of states, $N(E)$, of a cluster of muffin-tin potentials which has the form

$$N(E)=N_0(E)+\frac{2}{\pi}\sum_l(2l+1)\delta_l(E)+N_m(E), \tag{5}$$

where $N_0(E)$ is the integrated free-electron density of states, proportional to $E^{3/2}$. The second term, also structure independent, is a function of the phase shifts $\delta_l(E)$ of the single-site potential. $N_m(E)$ includes the modifications due to scattering among multiple sites. The approximate Fermi energy is determined by neglecting the structure-dependent term and solving the equation

$$Z=N(\epsilon_F)=N_0(\epsilon_F)+\frac{2}{\pi}\sum_l(2l+1)\delta_l(\epsilon_F), \tag{6}$$

where Z is the valence of the atom. The primary effect of the neglected multiple-site scattering term is to broaden the relatively narrow resonance in the $l=2$ phase shift into the d band. This implies that the maximum error in the approximate Fermi energy determined from Eq. (6) is smaller than half the d-band width, and that the approximation is least accurate for a nearly empty or nearly filled d band.

Figure 2 presents a comparison of energy levels calculated using these single-site renormalized-atom approximations for the $4d$ transition metals

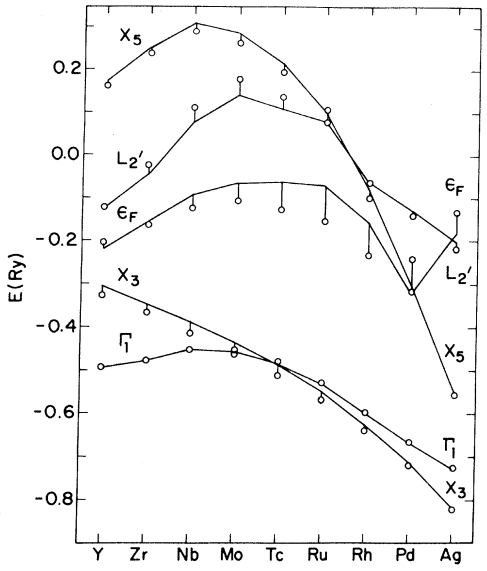

FIG. 2. Comparison of band calculation results for the 4*d* series (line) with the single-site renormalized-atom estimates (open circles) for the bottom of the *s* band (Γ_1), *p* band ($L_{2'}$), and *d* band (X_3), the top of the *d* band (X_5), and the Fermi energy (ϵ_F).

with corresponding fcc structure band calculation results based on the same potentials. The connected points and the open circles correspond, respectively, to the band results and the renormalized-atom estimates. The agreement for the band extrema is comparable to that obtained previously.[16] Γ_1 is predicted to within 0.005 Ry; $L_{2'}$, X_3, and X_5 are given to within 0.05 Ry or better. The Fermi-level agreement is less satisfactory with a maximum difference of 0.09 Ry for Ru. Part of the difference may be the result of inaccuracies in the Hodges scheme used to calculate ϵ_F from the band eigenvalues when it is applied to metals with such broad *d* bands, and part due to the crystal-structure dependence of the Fermi level. Pettifor[24] calculated the integrated density of states for the same potential on fcc, hcp, and bcc lattices and found the maximum difference $\epsilon_F^{\rm bcc}(N) - \epsilon_F^{\rm fcc}(N) \cong 0.02$ Ry for 6 electrons per atom.

These simple single-site approximations permit the gross features of the electronic structure of the metals to be quickly and easily calculated. They may be useful in obtaining estimates of the optical absorption edge of noble metals and their alloys, and in investigating other structure-independent electronic properties of metals and alloys.

III. COHESIVE ENERGY OF TRANSITION METALS

An earlier paper[15] outlined a method for calculating the cohesive energy of metals based on the renormalized atom, and presented estimates of the cohesive energy of the 3*d* and 4*d* transition metals. In this section we will present the results of full non-self-consistent calculations of the cohesive energy of 3*d* and 4*d* metals at their equilibrium density. Section IV will discuss calculations of the cohesive energy as a function of the volume per atom.

The cohesive energy of a transition metal can be expressed as the sum of five terms: (i) the atomic preparation energy required to excite a free atom from its ground state to the average energy of the $d^{n-1}s$ configuration appropriate to the solid[25]; (ii) the difference in total Hartree-Fock energy between the free $d^{n-1}s$ atom and the renormalized atom; (iii) the difference between the average energy of a free-electron band containing one electron and that of the renormalized atom *s* level; (iv) the change in one-electron en-

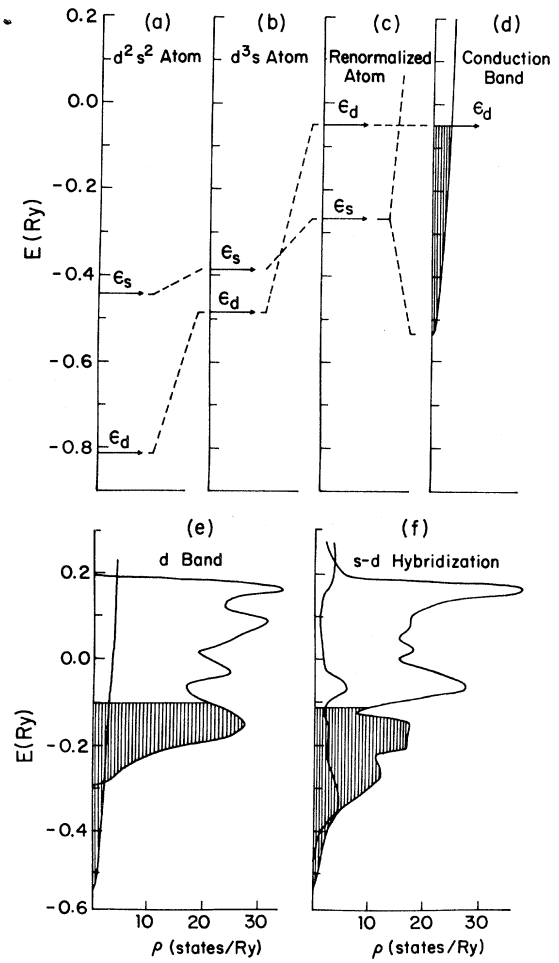

FIG. 3. Schematic electronic density of states for Ti at the various stages in the development of the crystalline density of states. The fcc structure is assumed for the crystal.

ergy per unit cell which results from the broadening of the renormalized atom d level in the d band; (v) the change in one-electron energy per unit cell due to the hybridization of the conduction and d bands. Appendix B contains a detailed description of the calculation of the various terms.

Figure 3 displays the density of states of Ti at each of the five stages in the development of the full crystalline density of states. The average energy of the d^3s configuration is 0.141 Ry above the d^2s^2 ground state. When the atom is renormalized, approximately 1.06 electrons are forced inside the Wigner-Seitz radius, decreasing the one-electron binding energy of the s and d orbitals. Because of the substantial cancellation of the double counted electron-electron Coulomb repulsion terms, the net energy cost of renormalization is only 0.064 Ry. In panel d the s level has been allowed to broaden into a free-electron band beginning at the crystalline Γ_1. The difference in one-electron energy between this band and the renormalized atom s level, ϵ_s^r, is −0.033 Ry. The largest contribution to the cohesion of a transition metal with a partially filled d band such as Ti is due to the broadening of the renormalized-atom d level into the d band.[1] This contribution can be calculated from the Hodges interpolation scheme[26] by artificially turning off the matrix elements which lead to finite d-band width. For Ti the contribution of d-band broadening calculated in this manner is −0.375 Ry. In the last panel the hybridization of the s and d bands has been turned on. Its effect is to push both s and d states away from the center of the d band. Since only states whose energy has been decreased are filled, the net effect is a bonding contribution of −0.161 Ry.

The calculated cohesive energy and its components for the $3d$ and $4d$ transition metals are displayed in Fig. 4. For each element the contributions from atomic preparation, renormalization, conduction-band formation, and d-band broadening plus s-d hybridization are indicated from left to right. The final calculated cohesive energy is represented by the filled block, while the experimental value[27] is marked by the open block. The calculations assume the experimental equilibrium metal density[28] and the fcc structure.

Examination of the trends of the various contributions shows that the atomic preparation energy is uniformly positive (except for the noble metals, where it vanishes), and is largest for elements with nearly half-filled d shells.

The renormalization contribution is typically of order 0.1 Ry or less. It peaks near the center of the row because the metallic Wigner-Seitz radius is smallest relative to the free-atom size for these elements leading to a maximal renormalization of atomic charge. The decrease between Cr and Mn is due to the sharp increase in Wigner-Seitz radius between them. There is an uncertainty of order 0.05 Ry in the renormalization energy for elements in the first two-thirds of the rows. For these elements the most weakly bound core p wave functions have non-negligible amplitude at the Wigner-Seitz radius. For example, slightly more than one-tenth of a Ti atomic $3p$ electron lies outside the Wigner-Seitz radius of the metal. The associated core renormalization effects have not been included here.

In these calculations the fcc structure has been used for all elements. The detailed d-band density of states is structure dependent, but the sum of one-electron energies which enters the cohesive energy is only weakly dependent on structure. For

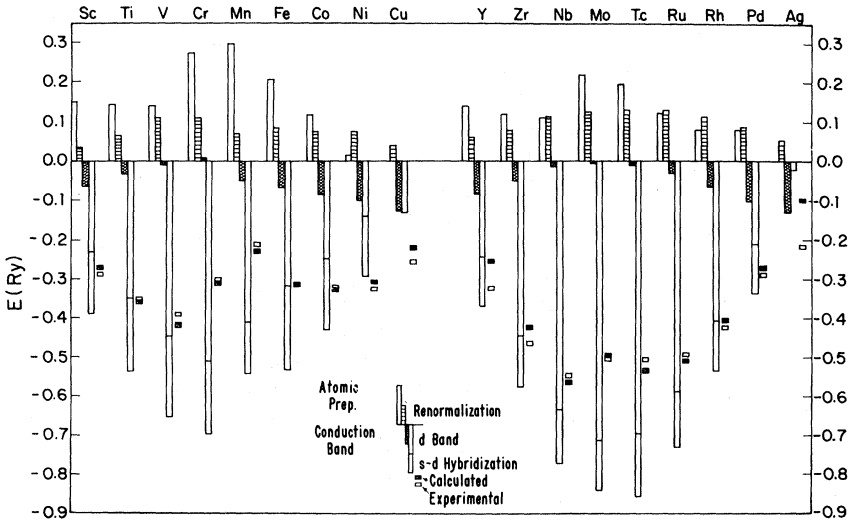

FIG. 4. Components of the cohesive energy for the $3d$ and $4d$ transition-metal rows. For each element the experimental value (Ref. 27) is denoted by the open box, the calculated value by the filled box.

example, Pettifor's[24] model calculations indicate that the maximum difference in cohesive energy among the fcc, bcc, and hcp structures for transition metals is only 0.03 Ry. In addition the assumption of a common structure has the advantage of removing a possible source of systematic error.

It is useful to separate the calculated change in the sum of one-electron energies between the renormalized atom and the crystal into the three components discussed above. Although this separation is obviously model dependent, the final calculated cohesive energy depends only on the sum of the terms and is independent of the detailed separation used. Appendix B presents details of the method used here.

The s-band broadening contribution [defined by Eq. (B15)] contributes to bonding, except for Cr. The magnitude of this term reflects the ratio of the Wigner-Seitz radius to the atomic radius. For midperiod elements the d bands pull the atoms close together compressing the conduction electrons. This raises the conduction band relative to the renormalized-atom s level and decreases the conduction-band bonding.

The remaining contributions to the cohesive energy result from the formation of the d bands and the hybridization of the conduction and d bands. From Fig. 4 it is clear that these terms are the largest part of the transition-metal cohesive energy. The nearly parabolic shape is a generic feature of the d-band contribution. In the simplest model the density of states of the d band is a rectangle of width W placed symmetrically about the one-electron level of the renormalized atom. For this model the d-band contribution to the cohesive energy for an element with N_d valence d electrons is

$$\Delta E_d(N_d) = (W/20)[N_d(10 - N_d)]. \tag{7}$$

It vanishes for a filled or empty band, and is a maximum for the half-filled band. If the true d-band density of states is more rounded than rectangular, the maximum of $\Delta E(N)$ will be smaller than predicted by Eq. (7). On the other hand, if the density of states is concentrated near the top and bottom of the band, the maximum will be greater.

The Heine-Hubbard[29] resonance model of the d band does not yield a clear-cut separation between the d-band broadening and s-d hybridization contributions to the cohesive energy. However, some idea of the relative magnitudes can be obtained by assuming a constant hybridization contribution, $\Delta E_{\rm hyb}$, and a d-band broadening term of the form of Eq. (7):

$$E(N) \cong \alpha(W/20)N_{\rm eff}(10 - N_{\rm eff}) + \Delta E_{\rm hyb}. \tag{8}$$

Here α is a scaling factor to account for the shape of the d band, and $N_{\rm eff} = N - N_0$. N is the total number of valence electrons and N_0 is chosen to place the maximum at the correct valence thereby fitting the d-band broadening contribution optimally. Using the first term in Eq. (8) as the d-band broadening contribution leads to the separation indicated in Fig. 4. The assumption of a nearly constant hybridization contribution is consistent with calculations based on the Hodges interpolation scheme.

The agreement between the calculated cohesive energies (filled boxes) and the experimental values (open boxes) is better than that found in the earlier renormalized-atom estimates.[30] For most elements the difference between theory and experiment is less than 0.03 Ry/atom. This agreement may be partly fortuitous in view of the uncertainty in some of the contributions. For example, many of the multiplets of the atomic $d^{n-1}s$ configuration for elements with nearly half-filled d shells are not identified[31] which tends to decrease the atomic preparation term. The uncertainty in the renormalization contribution of order 0.05 Ry was discussed above. The Brillouin-zone integration for the sum of valence one-electron energies could be in error by several hundredths of a rydberg. A conservative estimate of the uncertainty in the final calculated values would be ± 0.1 Ry. Because the errors for neighboring elements are correlated, the uncertainty in trends should be somewhat smaller.

On this scale of comparison the only severe problem is presented by the result for Ag, where the calculated cohesive energy is less than half the experimental value. This is apparently the result of the renormalized-atom potential placing the d band too low relative to the conduction band (see Fig. 2) thus reducing the hybridization contribution. The calculated optical absorption edge (taken as $\epsilon_F - L_3$) is 5.1 eV compared with the experimental value of 4 eV. Raising the d band relative to the conduction band would increase the hybridization contribution and improve the agreement with experiment. Other elements with relatively large errors are Cu (for which the calculated optical edge is in good agreement with experiment) in the 3d row, and Y and Zr at the beginning of the 4d row.

Self-consistent renormalized-atom calculations[32] of the cohesive energy of the 3d and 4d transition metals based on frozen-core atomic wave functions yield results in substantial agreement with the present non-self-consistent values. Self-consistency leads to a slightly more diffuse charge density which lowers the d bands relative to the conduction band. The effect on the cohesive energy is relatively small, less than 0.1 Ry for all elements but Fe, Co, and Ni for which the calculated

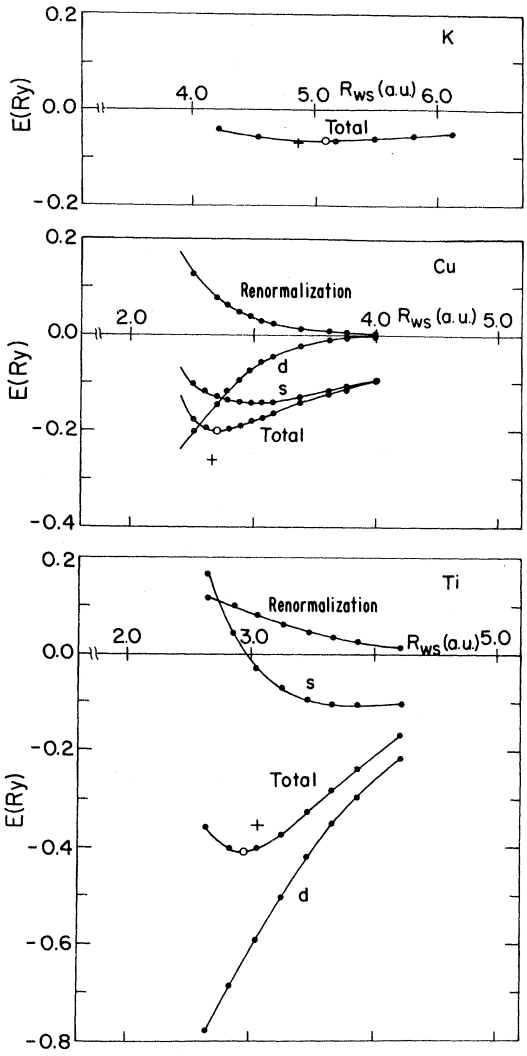

FIG. 5. Density dependence of the renormalization, s-band formation, and combined d-band broadening and s-d hybridization contributions to the cohesive energy of K, Ti, and Cu. The calculated total cohesive energy also contains the atomic preparation term which is independent of the density of the crystal. The open circles indicate the position of the calculated energy minima, while the crosses mark the experimental values (Ref. 34).

value is almost 0.2 Ry too small compared to experiment. The self-consistent results emphasize the insensitivity of the cohesive energy to relative shifts of the d and conduction bands caused by modified electron-electron terms.

These calculations do not include the contribution of the Van der Waals interaction which Rehr and co-workers[33] estimated to be 0.02 Ry/atom for Cu and 0.03 Ry/atom for Ag. These corrections are too small to explain all but a fraction of the discrepancy. The present success may encourage more precise calculations of the cohesive energy which will provide bounds on the net effect of many-body corrections.

IV. DENSITY DEPENDENCE OF THE COHESIVE ENERGY

The techniques described in Sec. III can be used to calculate the cohesive energy as a function of Wigner-Seitz radius. Figure 5 shows the density-dependent contributions and the total calculated cohesive energy (which includes the density-independent atomic preparation term) as a function of Wigner-Seitz radius for K, Cu, and Ti. The calculated points have been fitted to a polynomial in the Wigner-Seitz radius and this polynomial has been used to calculate the equilibrium Wigner-Seitz radius, the cohesive energy at the minimum, and the bulk modulus. The results are compared with experiment[34] in Table I and exhibited in the figure. The radius of Cu agrees with experiment to better than 2%. The Ti radius is small by about 3%, due in part to problems with the renormalization energy discussed below. The calculated radius for K is nearly 5% too large, but, as is seen in Fig. 5, the minimum is shallow. The cohesive energy of Cu is too small as it was in the calculations reported in Sec. III. The calculated bulk moduli agree with experiment to within about 20%.

As shown in the following discussion, the separation of the calculated cohesive energy into its components leads to a qualitative understanding of the competition between attractive and repulsive forces which determines the equilibrium density. The order-of-magnitude increases in the bulk modulus between K and the transition metals Ti and Cu will be shown to be the result of an attractive interaction between the d shells on neighboring atoms which reduces the Wigner-Seitz radius, compresses the conduction electrons, and increases the kinetic energy associated with localization.

The simplest example, K, can be calculated entirely from single-site renormalized-atom estimates. Because K has a single valence electron outside the core, the atomic preparation term vanishes. In addition, the renormalization energy reduces to the difference between the one-electron energy of the valence s orbital in the renormalized atom and the free atom [see Appendix B, Eq. (B13), with $n_d = 0$]. Finally, the occupied band structure is very nearly free-electron-like. As a result of these simplifications, the cohesive energy (in atomic units) can be expressed as

$$E_{\mathrm{coh}}(R_{\mathrm{WS}}) = \Gamma_1(R_{\mathrm{WS}}) + \tfrac{3}{5}k_F^2 - \epsilon_s^{\mathrm{atom}}. \tag{9}$$

Here Γ_1 is the energy of the bottom of the conduc-

TABLE I. Comparison of the calculated equilibrium Wigner-Seitz radius, cohesive energy, and bulk modulus for K, Cu, and Ti with experiment (Ref. 34).

	R_{min}(a.u.)		$E_{cohesive}$(Ry)		$K(10^{12}$ dynes/cm^2)	
	Expt.	Calc.	Expt.	Calc.	Expt.	Calc.
K	4.86	5.09	−0.0686	−0.066	0.32	0.3
Cu	2.67	2.71	−0.257	−0.20	13.1	11.5
Ti	3.05	2.95	−0.357	−0.38	10.5	12.2

tion band determined from the Wigner-Seitz boundary condition as described in Sec. II, and k_F is the free-electron Fermi momentum defined by

$$k_F = (9\pi/4)^{1/3} R_{WS}^{-1}. \tag{10}$$

The third term in Eq. (9) is the one-electron binding energy of the valence s orbital of the free atom.

As the Wigner-Seitz radius is decreased, Γ_1 is at first increasingly tightly bound because the valence charge density is compressed into a region of more attractive potential. At a Wigner-Seitz radius of about 4.35 a.u., Γ_1 passes through a minimum and then rises with decreasing radius as the kinetic energy cost of compressing the charge becomes dominant. The minimum of $\Gamma_1 + \frac{3}{5}k_F^2$ falls at a larger radius than that of Γ_1 because the Fermi-energy term is increasing positive as the radius is decreased. The bulk modulus, defined by

$$K = V\frac{\partial^2 E_{coh}}{\partial V^2} = \frac{1}{12\pi r}\left(\frac{\partial^2 E(r)}{\partial r^2} - \frac{2}{r}\frac{\partial E(r)}{\partial r}\right), \tag{11}$$

is small for K because the curvatures of both contributing terms in Eq. (9) are small.

It is not possible to calculate the cohesive energy of a noble or transition metal using this same simple renormalized-atom technique. The d-band broadening and s-d hybridization contributions both depend on the shape of the density of states, not merely the band extrema. Thus it is necessary to calculate the band structure as a function of density. The results for Ti and Cu are summarized in Fig. 6. Plotted are Γ_1, the limits of the d band, and the Fermi energy. For both elements the behavior of Γ_1 is similar to that described for K. The radius of the minimum of Γ_1 is smaller for Cu than for Ti reflecting the more compact Cu atomic s orbital. As the density is increased, the d bands broaden approximately as R^{-5} for Cu as predicted by the resonance model[29] but less rapidly for Ti where the narrow d-band approximation is less appropriate. For any radius the Ti d-band width is greater than that of Cu because of the greater overlap of the more diffuse Ti d orbitals. The Fermi energy in Cu remains above the top of the d band even when the Wigner-Seitz radius is decreased to 2 a.u., equivalent to a compression to more than twice the equilibrium density. Thus excitation of d electrons into higher states, which would signal the d-d exchange repulsion often ascribed to noble metals, is not observed in these calculations.

Returning to the Cu portion of Fig. 5, one finds, in fact, that the d electrons provide a bonding contribution through the s-d hybridization term. (The d-band broadening energy vanished for a filled d band.) Hybridization is increasingly bonding as the radius is decreased implying an attractive force between the atoms. The renormalization contribution is uniformly positive and increases with decreasing radius. The conduction-band formation energy goes through a shallow minimum out-

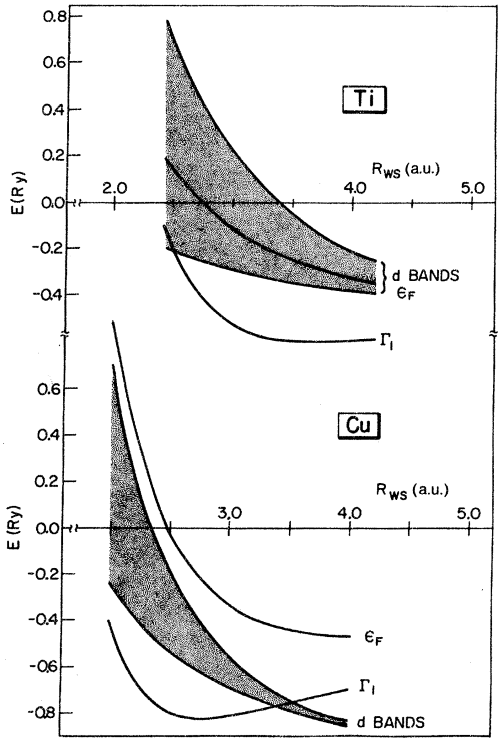

FIG. 6. Gross features of the Ti and Cu band structures as a function of Wigner-Seitz radius.

side the equilibrium radius. The Wigner-Seitz radius is thus determined by the competition between the attractive s-d hybridization contribution and the repulsive contribution of the other two terms. The dominant contribution to the bulk modulus[35] is the term $\Gamma_1 + \frac{3}{5}k_F^2$. If this were the only contribution, the bulk modulus evaluated at the calculated equilibrium radius would be 17×10^{12} dynes/cm^2, about 50% larger than the full calculated value give in Table I. The fact that the bulk modulus of Cu is a factor of 40 larger than that of K is due to the attractive s-d hybridization term which compresses the conduction electrons to a density region where both Γ_1 and k_F^2 have large positive curvatures.

This viewpoint is confirmed by treating Cu as an alkali metal. If one neglects the Cu d electrons and uses Eq. (9) to calculate the cohesive energy, one finds that the equilibrium Wigner-Seitz radius is increased to approximately 3.36 from 2.6 a.u., the cohesive energy is reduced to -0.11 from -0.20 Ry, and the bulk modulus falls by almost an order of magnitude from 11×10^{12} to 1.8×10^{12} dynes/cm^2. These results are in conflict with the quantum defect method calculations by Kambe[4] and the earlier cellular method studies by Fuchs.[3] To reproduce the experimental Wigner-Seitz radius, these authors found it necessary to invoke a repulsive interaction between the cores of neighboring atoms. The dominant contribution was assumed to come from the filled d shells. The extra repulsive term was needed because it had been assumed that the potential acting on a valence electron in the crystal was the same as that in the free atom. The compression of the valence charge density in the crystal, which Kambe and Fuchs neglected, results in a potential which is weaker as the atoms are brought closer together, thus increasing the equilibrium radius.

In the Ti panel of Fig. 5 the broad d band is reflected in the large s-d hybridization and d-band broadening contributions to the cohesive energy. The minimum in the calculated cohesive energy falls in a region where the conduction-band formation contribution is bending rapidly upward. Again this is the dominant term in the bulk modulus. Neither the renormalization energy nor the d-band terms shows significant curvature near the equilibrium density.

The larger uncertainties in the theoretical equilibrium Wigner-Seitz radius and bulk modulus for Ti as compared to K or Cu are the result of the weak binding of the $3p$ core state. As noted in Sec. III nearly 2% of the Ti atomic $3p$ charge lies outside the Wigner-Seitz radius, implying that this level should be renormalized, which was not done in the present calculations. Both the sign and the magnitude of this additional effect on the cohesive energy are therefore unclear.

These calculations of the cohesive energy versus Wigner-Seitz radius lead to several conclusions: (a) For all $3d$ and $4d$ transition and noble metals the formation of the d bands provides not only a bonding contribution (the magnitude of cohesive energy is increased) but also an attractive force (the bonding increases as the interatomic separation is decreased). (b) The "spring" which holds the atoms apart is primarily due to the kinetic energy of the conduction electrons. While they provide a bonding contribution (except in the case of Cr) the conduction electrons have been compressed into a density region in which the bonding decreases as the atoms are brought closer together.

V. CHEMICAL TREND OF THE WIGNER-SEITZ RADIUS

The calculations of the cohesive energy as a function of Wigner-Seitz radius for Cu and Ti shed light on the variation of the Wigner-Seitz radius across the transition metal rows. If the d electrons did not affect the binding, all metals in a period could be treated as alkali metals, and the equilibrium radius for each element would be determined by the minimum of $\Gamma_1 + \frac{3}{5}k_F^2$. This radius would decrease monotonically across a period reflecting the monotonic decrease of the size of the atomic valence s orbital due to the increasing nuclear charge. In fact, the d bonding effects are large and their influence modifies the expected variation of the metallic radius. As discussed above, the strength of the one-electron bonding due to the d electrons is proportional to the bandwidth, vanishes for an empty or filled d band, and is a maximum for a half-filled band. There is no corresponding simple expression for the s-d hybridization contribution. It will have a qualitatively similar behavior since the hybridization matrix element increases as the bandwidth increases, and the hybridization contribution is largest near a half-filled d band. Its effect, however, does not vanish for a filled band, but instead tails off with increasing valence. For example, it still contributes significantly for Cu. Including these d-band contributions will have the effect of decreasing the equilibrium Wigner-Seitz radius since their magnitude increases as the atoms are squeezed together. The decrease should be approximately parabolic as a function of the number of electrons per atom with the maximum effect near 6 electrons per atom. The final predicted curve of the Wigner-Seitz radius versus valence is then a skewed parabola, the parabola resulting from d bonding and s-d hybridization and the skewing from the increasing nuclear charge.

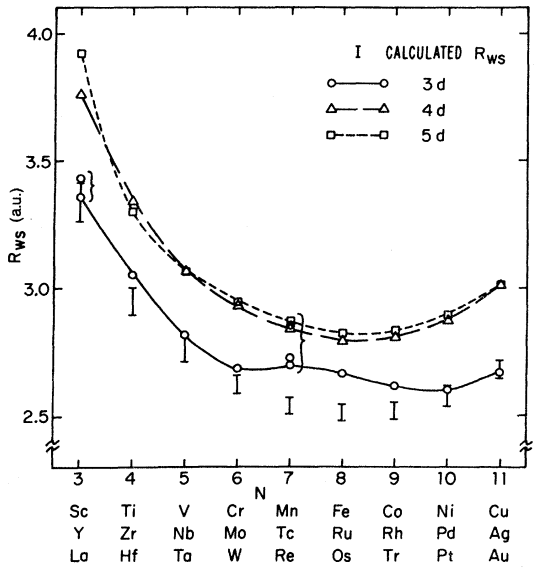

FIG. 7. Experimental Wigner-Seitz radius (Ref. 28) of the 3*d*, 4*d*, and 5*d* transition-metal series (open circles, triangles, and squares). The radii of the different allotropes are indicated for Sc and Mn. The error bars indicate the calculated Wigner-Seitz radius based on the density dependence of the Cu band structure.

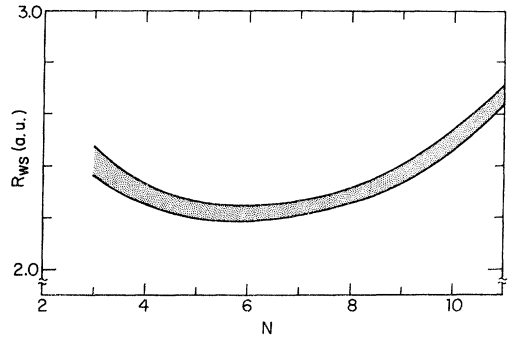

FIG. 8. The Wigner-Seitz radius calculated from the Cu density of states filled with N rather than 11 electrons. The shading indicates the uncertainty resulting from different approximations to the renormalization energy.

The curves in Fig. 7 show the valence dependence of the experimental[28] Wigner-Seitz radius in the three transition-metal periods. If more than one allotrope exists, the additional points represent the radius of the less dense structures. The bars indicate calculated values for the 3*d* row explained below. The experimental curves do show the expected behavior except in the 3*d* period between Mn and Ni where the radius is larger than one would estimate based on comparison with the 4*d* and 5*d* periods. Mn and to a lesser extent Sc are anomalous in having crystal structures with widely different densities. For the other elements the change in Wigner-Seitz radius between different structures is less than 1%.

Additional confirmation of this viewpoint can be gained from a simple model of the cohesive energy as a function of radius for all 3*d* transition metals based on the Cu calculations reported above. Let us suppose that it is legitimate to make the following physically plausible assumptions:

(i) For every 3*d* element Z there exists a measure of radial scale $R_{sc}(Z)$ and a constant $\alpha(Z) = R_{sc}(Z)/R_{sc}(\mathrm{Cu})$ such that (a) the renormalization energy at any radius R is equal to the Cu renormalization energy at the radius $R' = \alpha(Z)R$, and (b) the band structure at any radius R can be scaled onto the Cu band structure at radius $R' = \alpha(Z)R$.

(ii) A suitable choice of $R_{sc}(Z)$ for each element is the radius of maximum radial charge density of the Hartree-Fock atomic valence *s* orbital.

In order to utilize these assumptions, one first calculates $E(N,R)$, the cohesive energy of the Cu band structure as a function of the number of valence electrons N and the Wigner-Seitz radius R. Denote the minimum energy as a function of radius by $E_{min}(N)$ and the radius of the minimum as $R_{min}(N)$. Under the assumptions stated above, the equilibrium radius of the 3*d* element with N valence electrons is given by $R_{min}(N)[(R_{sc}(Z)/R_{sc}(\mathrm{Cu})]$. $R_{min}(N)$, the hypothetical radius of Cu with N rather than 11 electrons, is plotted in Fig. 8. The essentially parabolic dependence on N is a reflection of the *d*-band formation contributions described above. The result of correcting for the Z dependence of the radial scale factor[36] is plotted as the bars in Fig. 7. The general trend is reproduced quite well based simply on calculations of the Cu band structure and information about the size of the atoms. The smooth trend of the calculated results is more characteristic of the 4*d* and 5*d* series than the 3*d* series which exhibits a bump between Mn and Ni.[37]

This simple model works remarkably well. It is not surprising that the individual terms in the cohesive energy obey scaling relationships. The renormalization energy depends on the amount of free-atom charge outside the Wigner-Seitz radius, which will depend on the effective exponential decay length of the atomic charge density. Thus the Wigner-Seitz radius corresponding to a fixed amount of charge outside R_{WS} will be proportional to the decay length. Similarly one expects the *d*-band width to be proportional to the amount of overlap of *d* functions on neighboring atoms.

The surprising fact is that a model with a *single*

scale length for each element works as well as it does. One would expect that the density dependence of the renormalization energy and the bottom of the conduction band would be sensitive to the size of the s orbital, but that the d-band width would depend on the d orbital size. In fact, investigation of Fig. 6 indicates that scaling is not satisfied in detail. The Cu and Ti d-band widths scale as different powers of R; while the Cu d band is sufficiently narrow in the region 2.5–4 a.u. to be described by the Heine-Hubbard resonance model, the Ti d band is much broader and in fact scales with radius approximately as $R^{-3.5}$ rather than R^{-5}.

Perhaps a model using the atomic s orbital as the scale length is relatively successful because the equilibrium radius is determined by the radius at which the conduction-band formation energy bends up sharply, and this radius is relatively insensitive to the d band.

ACKNOWLEDGMENTS

We would like to thank A. R. Williams, J. F. Janak, and V. L. Moruzzi for useful comments and for communicating the results of their calculations prior to publication. J. B. Mann kindly provided a copy of his Hartree-Fock wave functions, and C. Froese Fischer made available the MCHF program. E. Esposito aided with the calculations for Ti as a function of density. One of us (HE) would like to express his thanks for the hospitality of the Physics Department of the University of Pennsylvania during the period when this paper was completed.

APPENDIX A: RENORMALIZED-ATOM AND OVERLAPPING-ATOM POTENTIALS

The renormalized-atom potential for an electron in orbital i is given by

$$V_i(\vec{r})\psi_i(\vec{r}) = \left[\sum_j \int_{WS} |\psi_j(\vec{r}')|^2 \frac{2}{|\vec{r}-\vec{r}'|} d^3r' - \frac{2Z}{r} - \sum_j \delta(m_{si}, m_{sj}) \frac{\psi_j(\vec{r})}{\psi_i(\vec{r})} \int_{WS} \psi_i^*(\vec{r}')\psi_j(\vec{r}') \frac{2}{|\vec{r}-\vec{r}'|} d^3r'\right] \psi_i(\vec{r}), \quad \text{(A1)}$$

where $\psi_i(\vec{r})$ is the renormalized wave function for the ith orbital whose radial part is defined in Eq. (1), Z is the nuclear charge, the δ-function restricts the third term to electrons with the same spin, and the integrals extend over the Wigner-Seitz sphere. The first two terms in Eq. (A1), the sum of the nuclear and direct electronic Coulomb potentials, are the Hartree potential. The third term is the exchange potential written in the Hartree localized exchange approximation.[21] The self-Coulomb interaction included here in the Hartree potential is cancelled by the self-exchange interaction. This is equivalent to including a Wigner-Seitz exchange-correlation hole: an electron on a neutral site with nuclear charge Z sees the potential due to $Z-1$ other electrons on the same site.

The most common prescription for constructing non-self-consistent potentials is to overlap atomic Hartree potentials and add an exchange potential proportional to the cube root of the overlapped charge density[19,38]:

$$V^{cryst}(\vec{r}) = V^{cryst}_{Hartree}(\vec{r}) + V^{cryst}_{exchange}(\vec{r}), \quad \text{(A2)}$$

where

$$V^{cryst}_{Hartree}(\vec{r}) = V^{atom}_{Hartree}(\vec{r}) + P_0\left\{\sum_{n\neq 0} V^{atom}_{Hartree}(\vec{r}-\vec{R}_n)\right\}, \quad \text{(A3)}$$

and

$$V^{cryst}_{exchange}(\vec{r}) = -6\alpha[(3/8)\rho^{cryst}(\vec{r})]^{1/3}, \quad \text{(A4)}$$

with

$$\rho^{cryst}(\vec{r}) = \rho^{atom}(\vec{r}) + P_0\left\{\sum_{n\neq 0} \rho^{atom}(\vec{r}-\vec{R}_n)\right\}. \quad \text{(A5)}$$

The notation $P_0\{\cdots\}$ indicates that only the spherically symmetric part of the sum is retained. The parameter α is usually given a value between $\alpha = 1$ suggested by Slater[20] and $\alpha = \frac{2}{3}$ as derived by Gaspar[39] and Kohn and Sham.[22] Schwarz[40] has tabulated the value of α for which the total energy of a free atom using an exchange potential of the form of Eq. (A4) is equal to the Hartree-Fock energy for the elements H through Nb.

Figure 9 compares the energy bands for Cu along the [100] direction using the renormalized-atom potential and overlapping-atom potentials with $\alpha = 1$ and $\alpha = \frac{2}{3}$. The three potentials were constructed from the same frozen-core Cu $d^{10}s$ Hartree-Fock atomic wave functions. There are striking differences both in the energy of the d bands relative to the conduction band, and in the energy of the complex of bands relative to the atomic zero of potential.

Three factors contribute to these differences: (1) the treatment of exchange, (2) the radial dependence of $\delta\rho(\vec{r}) = \rho^{cryst}(\vec{r}) - \rho^{atom}(\vec{r})$, and (3) the choice of the zero of the Hartree potential in the crystal. If one compares the exchange potential defined by Eq. (A4) with $\alpha = 1$ and the renormalized-atom exchange potential defined by

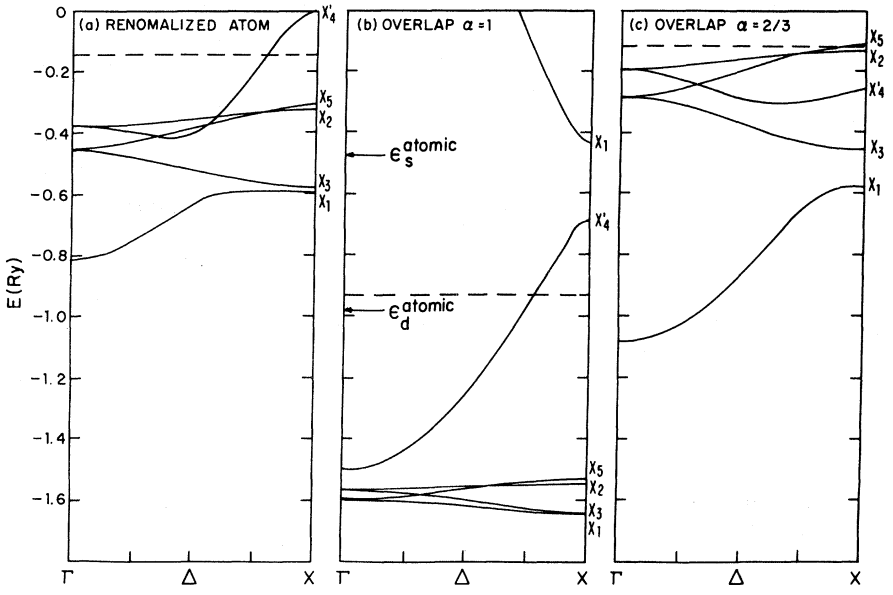

FIG. 9. Energy bands for Cu along the [100] direction calculated from the renormalized-atom potential (a), and overlapping-atoms potentials with exchange-correlation parameter $\alpha=1$ (b) and $\alpha=\frac{2}{3}$ (c). Also indicated are the free-atom Hartree-Fock one-electron energies for the $3d$ and $4s$ orbitals.

$$V_{\text{exch}}^{\text{RA}}(\vec{r}) = V^{\text{RA}}(\vec{r}) - V_{\text{Hartree}}^{\text{RA}}(\vec{r}) \ , \tag{A6}$$

one finds that in the region where the d functions are large they differ by less than 0.2 Ry. Similar behavior is observed in the $4s$ raidal region.[41] The difference between panels (a) and (b) of Fig. 9 therefore is not due to the differing treatment of exchange.

Next consider $\delta\rho(\vec{r})$, the difference between the crystalline and atomic charge density. Since a Wigner-Seitz cell in the crystal is neutral, the integral of $\delta\rho(\vec{r})$ over the cell, Q_{out}, must be the same for the renormalized atom and for overlapping atoms. The radial dependence is quite different. For $\rho^{\text{cryst}}(\vec{r})$ defined by Eq. (A5), $\delta\rho(\vec{r})$ is small for small r and strongly peaked in the outer portions of the cell. For the renormalized atom

$$\delta\rho(\vec{r}) = \sum_{\substack{\text{orbitals}\\ i}} (N_i - 1) n_i \left| \psi^{\text{atom}}(\vec{r}) \right|^2 \ , \tag{A7}$$

where N_i is the normalization constant for the ith orbital defined by Eq. (2), n_i is the number of electrons occupying the orbital, and $|\psi_i^{\text{atom}}(\vec{r})|^2$ is the atomic charge density of the orbital. The dominant contribution to this sum for a transition metal comes from the valence s orbital. Thus $\delta\rho(\vec{r})$ will exhibit the same radial dependence as the s orbital. This implies that the largest value of $\delta\rho(\vec{r})$ occurs in the region of the core oscillations, and that $\delta\rho(\vec{r})$ is essentially constant over the outer portions of the Wigner-Seitz cell.

The difference between the crystalline and atomic Hartree potentials can be calculated from $\delta\rho$:

$$V_{\text{Hartree}}^{\text{cryst}}(r) - V_{\text{Hartree}}^{\text{atom}}(r) = \frac{8\pi}{r}\int_0^r \delta\rho(x)x^2\,dx + 8\pi\int_r^{R_{\text{WS}}}\left[\frac{\delta\rho(x)}{x}\right]x^2\,dx + C \ . \tag{A8}$$

Figure 10 displays this difference for the renormalized atom and for overlapping atoms. To zeroth order the overlapping-atoms curve is constant, consistent with $\delta\rho$ strongly peaked near R_{WS}. If $\delta\rho$ itself is constant, the solution of Eq. (A8) is

$$\delta V(r) = \frac{Q_{\text{out}}}{R_{\text{WS}}}\left[3 - (r/R_{\text{WS}})^2\right] + C \ , \tag{A9}$$

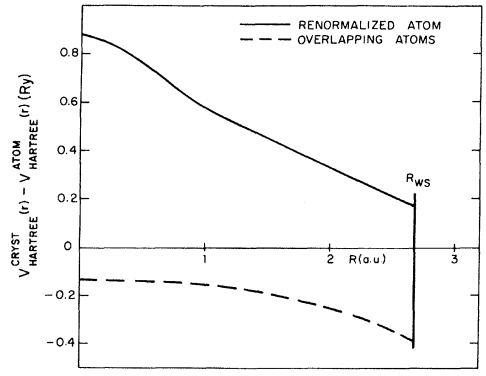

FIG. 10. Difference between the crystalline Hartree potential and the atomic Hartree potential as a function of radius. The shape of the curves reflects the radial dependence of the difference between the crystalline and atomic charge densities.

which is a good representation of the renormalized-atom curve, at least in the region $r>1$. Because most of the d charge lies in the region $r=1$ while most of the conduction charge lies outside $r=1.5$, Fig. 10 implies that the d bands will lie higher relative to the conduction band for the renormalized-atom potential than for the overlapping atoms potential as is seen in Fig. 9.

Figure 11 compares the Hartree potentials for the free atom with the two models of the crystalline Hartree potential defined above. The potentials are plotted as $2rV(r)$ to emphasize the large-radius region. The renormalized-atom curve is always above that for the free atom, the overlapping atoms curve is always below. This is a result of a different choice of the constant of integration in Eq. (A8). For the renormalized atom, C is chosen to give $V^{\text{cryst}}_{\text{Hartree}}(R_{\text{WS}})=0$. For overlapping Hartree potentials, all of which are negative, the sum will be more negative than any of the individual potentials. Thus, even though a Wigner-Seitz cell is neutral, the Hartree potential at the surface of the cell is not zero. This is equivalent, in a bounded crystal, to a nonzero surface dipole layer as defined by Seitz.[42] The difference between $V^{\text{RA}}_{\text{Hartree}}(R_{\text{WS}})$ and $V^{\text{overlap}}_{\text{Hartree}}(R_{\text{WS}})$, 0.55 Ry, is the surface dipole layer one would obtain by modelling the crystal charge density with overlapping atoms.

The difference between the two models of the Hartree potential can be partly offset by varying the strength of the exchange potential in Eq. (A4) as is demonstrated in panel (c) of Fig. 9. Reducing the strength of exchange decreases the binding of all states, but because $\rho(r)$ and thus $V_{\text{exch}}(r)$ is larger in the region of the d electrons, reducing α has the effect of raising the d bands relative to the conduction bands.

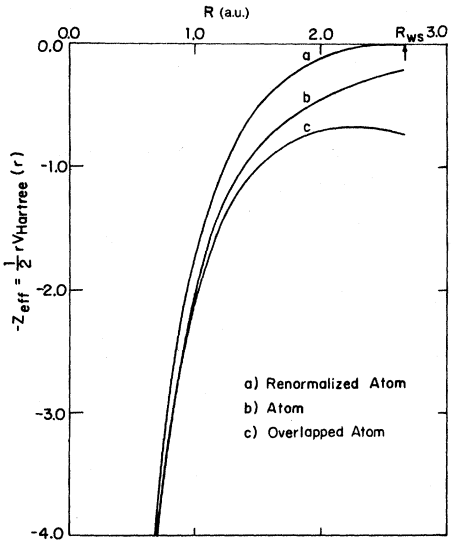

FIG. 11. "Effective nuclear charge" as a function of radius for (b) atomic Cu and for (a) the renormalized and (c) the overlapping atoms prescription for calculating the Hartree potential of the crystal.

APPENDIX B: COHESIVE-ENERGY CALCULATIONS

The calculations of the cohesive energy of the transition metals rely on the use of the renormalized atom to calculate: (a) the change of the two-electron (Coulomb and exchange) integrals between the solid and the free atom, and (b) the effective one-electron potential to be used in an energy-band calculation. The resulting cohesive energy is given by

$$\begin{aligned}\Delta E =&\Delta E \text{ (atomic preparation)}\\ &+\Delta E \text{ (renormalization)}\\ &+\Delta E_{\text{one-electron}} \text{(band formation)} .\end{aligned} \tag{B1}$$

The first term is the energy necessary to excite an atom from its ground state to the average of the $d^{n-1}s$ valence electron configuration where n is the total number of valence electrons. This quantity is determined by averaging the energy of the observed multiplets[31] of the $d^{n-1}s$ configuration. For example, the average energy of the d^9s configuration of Ni relative to the $^3F(d^8s^2)$ ground state, ΔE (atomic prepartion), is 0.013 Ry.

This procedure could not be used for Tc because too many of the multiplets of the d^6s configuration are not cataloged for a reliable average to be calculated. Instead the trends of the four quantities

$$\begin{aligned}&(d^{n-1}s)_{\text{av}}-(d^{n-2}s^2)_{\text{min}} ,\\ &(d^{n-1}s)_{\text{av}}-(d^{n-2}s^2)_{\text{av}} ,\\ &(d^{n-2}s^2)_{\text{av}}-(d^{n-2}s^2)_{\text{min}} ,\\ &(d^{n-1}s)_{\text{av}}-(d^{n-1}s)_{\text{min}} ,\end{aligned} \tag{B2}$$

in the $3d$ sequence Cr-Mn-Fe and the $5d$ sequence W-Re-Os were interpolated to the sequence Mo-Tc-Ru. In these expressions $(\cdots)_{\text{av}}$ denoted the energy of the average of the configuration, and $(\cdots)_{\text{min}}$ denotes the energy of the lowest multiplet. The atomic preparation energy for Tc, the difference between $(d^6s)_{\text{av}}$ and the $^6S(d^5s^2)$ ground state, can be estimated from the following expressions (the number in parentheses is the resulting value of the atomic preparation energy):

$$\begin{aligned}&(d^6s)_{\text{av}}-(d^5s^2)_{\text{min}} , \quad (0.206 \text{ Ry})\\ &[(d^6s)_{\text{av}}-(d^5s^2)_{\text{av}}]+[(d^5s^2)_{\text{av}}-(d^5s^2)_{\text{min}}] ,\\ &\qquad\qquad (0.209 \text{ Ry})\\ &[(d^6s)_{\text{av}}-(d^6s)_{\text{min}}]+[(d^6s)_{\text{min}}-(d^5s^2)_{\text{min}}] ,\\ &\qquad\qquad (0.183 \text{ Ry}) .\end{aligned} \tag{B3}$$

An average value of 0.2 Ry was used for Fig. 4.

The second term in Eq. (B1) is the difference in total Hartree-Fock energy between the free atom and the renormalized atom.[43] This can be written in the form

$$\Delta E \text{ (renormalization)} = \sum_i n_i \left(\Delta I_i + \tfrac{1}{2}(n_i - 1)\Delta U_{ii} + \frac{1}{2} \sum_{j \neq i} n_j \Delta U_{ij} \right) , \quad \text{(B4)}$$

where the sums run over the occupied orbitals, n_i is the occupation number of the ith orbital, and Δ denotes the difference between the renormalized-atom and the free-atom value. I_i is the one-electron kinetic and nuclear potential energy integral

$$I_i = I(nl) = \int_0^R P_{nl}^*(r) \left(-\frac{d^2}{dr^2} + \frac{l(l+1)}{r^2} - \frac{2Z}{r} \right) P_{nl}(r)\, dr , \quad \text{(B5)}$$

where n and l are the quantum numbers of the ith orbital. The upper limit of the integration is the renormalization radius (infinite for the free atom), $P_{nl}(r)$ is the radial function normalized by

$$\int_0^R [P_{nl}(r)]^2 dr = 1 , \quad \text{(B6)}$$

and Z is the nuclear charge. The unit of energy is the rydberg. The kinetic energy integration for the renormalized atoms does *not* include a contribution from the truncation of the wave functions at R_{WS}. U_{ij} is the average-of-configuration weighted sum of Coulomb and exchange integrals.[44] For example, for two d electrons with the same principal quantum number

$$U_{ii} = U(nd, nd) = F^0(nd,nd) - \tfrac{2}{63}\{\tfrac{1}{5}[F^2(nd,nd) + 4G^2(nd,nd)] + \tfrac{1}{9}[F^4(nd,nd) + 8G^4(nd,nd)]\} . \quad \text{(B7)}$$

For two d electrons in different shells

$$U_{ij} = U(nd, n'd) = F^0(nd,n'd) - \tfrac{1}{10} G^0(nd,n'd) - \tfrac{1}{35}[G^2(nd,n'd) + G^4(nd,n'd)] . \quad \text{(B8)}$$

Similar expressions are given by Slater[44] for the other two-electron integrals. In these expressions $F^k(nl,n'l')$ is the Coulomb integral defined by

$$F^k(nl,n'l') = \int_0^R \int_0^R P_{nl}^*(r_1) P_{n'l'}^*(r_2) \frac{2r_<^k}{r_>^{k+1}} \times P_{nl}(r_1) P_{n'l'}(r_2)\, dr_1\, dr_2 , \quad \text{(B9)}$$

and $G^k(nl,n'l')$ the exchange integral

$$G^k(nl,n'l') = \int_0^R \int_0^R P_{nl}^*(r_1) P_{n'l'}^*(r_2) \frac{2r_<^k}{r_>^{k+1}} \times P_{nl}(r_2) P_{n'l'}(r_1)\, dr_1\, dr_2 . \quad \text{(B10)}$$

For the case $nl = n'l'$, these definitions imply $G^k = F^k$.

If we define core levels (C) to be those for which the integrated charge density outside the Wigner-Seitz sphere is negligible, and assume that the kinetic energy of these orbitals is the same in the solid as in the atom, then for $i \in C$, $\Delta I_i = \Delta U_{ii} = 0$. After separating the sums in Eq. (B4) into contributions from core and noncore orbitals, Eq. (B4) can be rewritten as

$$\Delta E \text{ (renormalization)} = \sum_{i \notin C} n_i \left(\Delta\epsilon_i - \tfrac{1}{2}(n_i - 1)\Delta U_{ii} - \frac{1}{2} \sum_{\substack{j \neq i \\ j \in C}} n_j \Delta U_{ij} \right) . \quad \text{(B11)}$$

Here

$$\Delta\epsilon_i = \Delta I_i + (n_i - 1)\Delta U_{ii} + \sum_{j \neq i} n_j \Delta U_{ij} \quad \text{(B12)}$$

is the change in the Hartree-Fock one-electron energy. Note that Eq. (B11) does not explicitly contain core integrals. If one assumes that only the outermost s and d orbitals are affected by renormalization, then the result (B12) for the $d^{n-1}s$ configuration can be rewritten as

$$\Delta E \text{ (renormalization)} = \Delta\epsilon_s + n_d[\Delta\epsilon_d - \tfrac{1}{2}(n_d - 1)\Delta U_{dd} - \Delta U_{sd}] . \quad \text{(B13)}$$

This form exhibits the large cancellation between the one-electron energy shifts and the two-electron terms. Table II lists the various components of this equation for Cu. The degree of cancellation between $\Delta\epsilon_d$ and the change in valence Coulomb integrals is similar for other transition metals.

The final contribution to Eq. (B1) is the change in total one-electron energy due to the broadening of the sharp renormalized-atom levels into bands

TABLE II. Components of Eq. (B13) for Cu renormalized to its equilibrium density.

$\Delta\epsilon_s$	0.100 Ry
$\Delta\epsilon_d$	0.568 Ry
ΔU_{dd}	0.0524 Ry
ΔU_{sd}	0.335 Ry
ΔE(ren.)	0.075 Ry

$\Delta E_{\text{one electron}}$ (band formation)

$$= \int_{-\infty}^{\epsilon_F} E\rho(E)\,dE - \sum_i n_i \epsilon_i^r \ , \quad \text{(B14)}$$

where $\rho(E)$ is the one-electron density of states resulting from an energy band calculation and ϵ_i^r is the renormalized-atom one-electron energy for the ith valence orbital defined in Eq. (B12).

In practice the one-electron energy sum for the band is calculated either by fitting the parameters of the combined interpolation scheme[26] to symmetry-points eigenvalues, or by the special points averaging method[45] using ten low-symmetry points in the irreducible wedge of the Brillouin zone. The two methods yield the same one-electron sum to within about 0.02 Ry even though the rms error of the interpolation fit is relatively large (>0.02 Ry) for the broad d bands in the center of the periods.

The separation of $\Delta E_{\text{one electron}}$ into its various components is defined as follows:

$$\Delta E_{s\text{-band formation}} = \Gamma_1 + \tfrac{3}{5} k_F^2 - \epsilon_s^r \ , \quad \text{(B15)}$$

where Γ_1 is the lowest state in the conduction band determined from either Wigner-Seitz boundary conditions as in Eq. (3) above or a band-structure calculation, and k_F^2 is calculated from the free-electron model

$$k_F^2 = (3\pi^2 N/V)^{2/3} \ . \quad \text{(B16)}$$

The partitioning of the remainder of $\Delta E_{\text{one-electron}}$ into d-band broadening and s-d hybridization terms is accomplished either by using the combined interpolation scheme or by assuming that the hybridization contribution is constant near the middle of a row and fitting its magnitude and an *ad hoc* d-band broadening term to the calculated sum. When using the interpolation Hamiltonian, the two terms are calculated by successively turning off the parameters which produce s-d hybridization and d-band width:

$$\Delta E_{\text{hybrid}} = E(\text{full}) - E(\text{no hybrid}) \ , \quad \text{(B17)}$$

$$\Delta E_{d \text{ width}} = E(\text{no hybrid}) - E(\text{no hybrid, no } d \text{ width}) \ , \quad \text{(B18)}$$

where E is the band sum of one-electron energies.

Due to difficulties fitting the parameters of the Hodges model to the broad d bands in the middle of the 4d series, this method could not be used for the partitioning indicated in Fig. 4 although it was used for Figs. 3 and 5. For Fig. 4 the hybridization contribution was assumed to be essentially constant for the elements with 3 to 9 valence electrons per atom, as indicated by interpolation Hamiltonian calculations, with the constant chosen to give a d-band broadening contribution proportional to the product of the d-band width and a quadratic function of $N_d - 5$, where N_d is the number of d electrons per atom. For the 3d elements this gave $N_d = N - 1.3$, for the 4d elements $N_d = N - 1.5$. The resulting partitioning should be viewed as semiquantitative at best. However, as emphasized in the main body of the paper, the total cohesive energy is independent of the partitioning chosen.

---

*Research supported in part by the NSF through Grants No. DMR72-02977 and DMR76-01111.

†Research performed under the auspices of the U.S. Energy Research and Development Administration.

[1]E. Wigner and F. Seitz, Phys. Rev. 43, 804 (1933); 46, 509 (1934).

[2]H. Brooks, Nuovo Cimento Suppl. 7, 165 (1958).

[3]K. Fuchs, Proc. R. Soc. Lond. A 151, 585 (1935); A 153, 622 (1936).

[4]K. Kambe, Phys. Rev. 99, 419 (1955).

[5]F. Stern, Phys. Rev. 116, 1399 (1959).

[6]B. Segall, Phys. Rev. 125, 109 (1962).

[7]G. A. Burdick, Phys. Rev. 129, 138 (1963).

[8]J. Friedel, Proc. Phys. Soc. B 65, 769 (1952).

[9]N. F. Mott, Rept. Prog. Phys. 25, 218 (1962); Adv. Phys. 13, 325 (1964).

[10]J. Friedel, in *The Physics of Metals I*, edited by J. M. Ziman (Cambridge U. P., Cambridge, 1969).

[11]F. Ducastelle and F. Cyrot-Lackmann, J. Phys. Chem. Solids 32, 285 (1971).

[12]J. Kollar and G. Solt, J. Phys. Chem. Solids 33, 651 (1972); 35, 1121 (1974). The authors are grateful to Professor Solt for pointing out that the second article referred to concluded that the interaction of neighboring d shells in Cu is slightly attractive.

[13]D. A. Liberman, Phys. Rev. B 2, 244 (1971), Cu; F. W. Averill, Phys. Rev. B 4, 3315 (1971), Cs; Phys. Rev. B 6, 3637 (1972), alkali metals; S. B. Trickey, F. W. Averill, and F. R. Green, Jr., Phys. Lett. A 41, 385 (1972), Ar; T. M. Hattox, J. B. Conklin, J. C. Slater, and S. B. Trickey, J. Phys. Chem. Solids 34, 1627 (1973), V; E. C. Snow, Phys. Rev. B 8, 5391 (1973), Cu; V. L. Moruzzi, J. F. Janak, and A. R. Williams (unpublished), K→Ga, Rb→In.

[14]R. E. Watson, H. Ehrenreich, and L. Hodges, Phys. Rev. Lett. 24, 829 (1970).

[15]R. E. Watson and H.Ehrenreich, Comments Solid State Phys. 3, 109 (1970).

[16]L. Hodges, R. E. Watson, and H. Ehrenreich, Phys. Rev. B 5, 3953 (1972).

[17]O. K. Andersen, Phys. Rev. B 12, 3060 (1975).

[18]K.-F. Berggren, Phys. Rev. B 6, 2156 (1972); K.-F. Berggren, S. Manninen, and T. Paakkari, Phys. Rev. B 8, 2516 (1973).

[19]L. F. Mattheiss, Phys. Rev. 133, A1399 (1964).

[20]J. C. Slater, Phys. Rev. 81, 385 (1951).

[21]D. R. Hartree, *The Calculation of Atomic Structure* (Wiley, New York, 1957).
[22]W. Kohn and L. J. Sham, Phys. Rev. 140, A1133 (1965).
[23]P. Lloyd, Proc. Phys. Soc. 90, 207 (1967).
[24]D. G. Pettifor, J. Phys. C 3, 367 (1970).
[25]E. C. Snow and J. T. Waber, Acta Metall. 17, 623 (1969).
[26]L. Hodges, Ph.D. thesis (Harvard University, 1966) (unpublished); H. Ehrenreich and L. Hodges, Methods Comput. Phys. 8, 149 (1968).
[27]The values of the experimental cohesive energy for all elements other than Sc, Tc, and Pd are taken from R. Hultgren, R. L. Orr, and K. K. Kelley, *Selected Values of Thermodynamic Properties of Metals and Alloys* (Wiley, New York, 1963). The values for Sc and Pd are from R. E. Honig and D. A. Kramer, RCA Rev. (Radio Corp. Am.) 30, 295 (1969), and the value for Tc is from O. H. Krikorian, J. H. Carpenter, and R. S. Newbury, High Temp. Sci. 1, 313 (1969).
[28]W. B. Pearson, *A Handbook of Lattice Spacings and Structures of Metals and Alloys* (Pergamon, New York, 1958).
[29]V. Heine, Phys. Rev. 153, 673 (1967); J. Hubbard, Proc. Phys. Soc. 92, 921 (1967).
[30]The present results are improvements on the previous estimates of Ref. 15 in two important respects. First, in the earlier estimates the atomic preparation energy was calculated by adding to the Slater-Condon-Racah theory value for the energy of the center of gravity of the $d^{n-1}s$ configuration relative to its lowest multiplet the energy of the lowest $d^{n-1}s$ level (from Ref. 31). In the present calculations the atomic preparation energy was calculated from the average of all experimentally observed multiplets of the $d^{n-1}s$ configuration (see Appendix B). Second, the previous estimates assumed a constant hybridization contribution to the cohesive energy for each row based on calculations for Ni, Cu, and Ag and used the d-band broadening contribution from Ref. 11. The present results of Fig. 4 are based on full band calculations for each element.
[31]*Atomic Energy Levels*, edited by C. E. Moore (National Bureau of Standards Circular 467, 1952).
[32]R. E. Watson (unpublished).
[33]J. J. Rehr, E. Zaremba, and W. Kohn, Phys. Rev. B 12, 2062 (1975).
[34]The experimental values of the cohesive energy and Wigner-Seitz radius for K, Ti, and Cu are from Refs. 27 and 28, respectively. The values of the bulk modulus are from K. A. Gschneidner, Jr., in *Solid State Physics*, edited by F. Seitz and D. Turnbull (Academic, New York, 1965), Vol. 16, p. 275.
[35]The importance of band-structure contributions to the bulk modulus has been discussed previously by N. W. Ashcroft and D. C. Langreth, Phys. Rev. 155, 682 (1967).
[36]The radial scale factors used to transfer the results of Fig. 8 to Fig. 7 were taken as the radius of maximum radial charge density of the Hartree-Fock 4s orbitals for atoms in the $d^{n-1}s$ configuration. Quite similar results are obtained using either the average or rms radius of the 4s orbital, or the screening rules from J. C. Slater, Phys. Rev. 36, 57 (1930).
[37]The discrepancy between the 3d row and the 4d and 5d rows may be viewed either as a break between two smooth curves, Sc-Cr and Mn-Cu, or as an anomalously large Wigner-Seitz radius for the elements Mn-Ni. Partial support for the latter viewpoint is given by the observation that the formation of an ordered spin state increases the interatomic separation. M. Shiga, in AIP Conf. Proc., Vol. 18, edited by C. D. Graham and J. J. Rhyne (AIP, New York, 1974) noted a correlation between lattice constant and magnetic moment in binary solid solutions of 3d metals. He found that the increase in Wigner-Seitz radius could be approximated by δR (a.u.) $= 0.03 \langle|\mu|\rangle$. Applying this to the pure elements using the average moments for for Fe, Co, and Ni one finds an increase in radius of 0.07, 0.05, and 0.01 a.u., respectively, which would remove most of the discrepancy. The case of Mn is unresolved. Further support for coupling between lattice constant and nonzero magnetic moments is provided by self-consistent spin polarized calculations of the cohesive energy of 3d transition metals by J. F. Janak (unpublished).
[38]T. L. Loucks, *The Augmented Plane Wave Method* (Benjamin, New York, 1967), Chap. 3.
[39]R. Gaspar, Acta Phys. Hung. 3, 263 (1954).
[40]K. Schwarz, Phys. Rev. B 5, 2466 (1972).
[41]C. D. Gelatt, Jr., Ph.D. thesis (Harvard University, 1974) (unpublished).
[42]F. Seitz, *The Modern Theory of Solids* (McGraw-Hill, New York, 1940), p. 397.
[43]Three different programs were used to generate the Hartree-Fock atomic wave functions. For the calculations represented by Fig. 4, the 3d wave functions were frozen-core calculations with the core taken from calculations for the d^{n-1} ions [R. E. Watson, Technical Report No. 12, Solid-State and Molecular Theory Group, Massachusetts Institute of Technology (unpublished)]. For Nb, Mo, Ru, Rh, and Ag the wave functions are numerical Hartree-Fock results (no frozen core) from J. B. Mann, LA-3690 and LA-3691, Los Alamos Scientific Laboratory reports (1967) (unpublished) and private communication. For Y, Zr, Tc, and Pd, C. Froese Fischer's MCHF 72 program [Comput. Phys. Commun. 4, 107 (1972)] was used. The K and Ti lattice constant calculations in Fig. 5 are based on MCHF 72 wave functions, while the Cu calculations used frozen-core wave functions.
[44]J. C. Slater, *Quantum Theory of Atomic Structure* (McGraw-Hill, New York, 1960), Vol. II, pp. 18–30.
[45]A. Baldereschi, Phys. Rev. B 7, 5212 (1973); D. J. Chadi and M. L. Cohen, Phys. Rev. B 8, 5747 (1973).